

Experimental Determination of the Cr–C₂Cl₄ Bond Dissociation Enthalpy in Cr(CO)₅(C₂Cl₄): Quantifying Metal–Olefin Bonding Interactions

David L. Cedeño[†] and Eric Weitz*

Contribution from the Department of Chemistry, Northwestern University, Evanston, Illinois 60208-3113

Received July 6, 2001

Abstract: The bond dissociation enthalpy for the Cr–C₂Cl₄ bond in gas-phase Cr(CO)₅(C₂Cl₄) has been determined to be 12.8 ± 1.6 kcal/mol using transient infrared spectroscopy. The results of a density functional theory-based energy decomposition analysis are used to quantify the metal–olefin bonding interactions in terms of the bonding description provided by the Dewar–Chatt–Duncanson model (σ donation and back-bonding). The bond energy decomposition analysis reveals that metal–olefin bond strengths can be strongly influenced by the Pauli repulsion energy and by the energy necessary to deform the olefin and the metal-centered moiety from their equilibrium geometries to their geometry in the final complex. Further, a comparison between the metal–olefin bond strengths and the magnitude of the electronic interactions demonstrates that the energy associated with these deformations is the determining factor in the trends in bond enthalpies in the series of complexes Cr(CO)₅(C₂X₄) (X = H, F, Cl). Though deformation of the Cr(CO)₅ moiety contributes to the overall deformation energy, the major contribution involves deformation of the olefin. This occurs as a consequence of rehybridization of the olefin as a result of metal–olefin back-bonding. The results are discussed in terms of the Dewar–Chatt–Duncanson model, which provides the accepted qualitative description of bonding in organometallic olefin complexes.

I. Introduction

Olefin–metal complexes play an important role in organometallic chemistry. They are involved in a variety of chemical transformations, including catalytic processes such as olefin isomerization, hydrogenation, and epoxidation.^{1–3} Because these reactions can involve the formation and/or cleavage of a metal–olefin bond, an understanding of metal–olefin interactions is necessary for a rational design of suitable catalysts for such processes. The Dewar–Chatt–Duncanson (DCD) model^{4,5} is widely used to describe metal–olefin bonding interactions. In this qualitative model, two synergistic bonding interactions contribute to the metal–olefin bond. The π HOMO of the olefin donates electron density to the metal's empty dsp-hybrid LUMO in what is called σ donation. The metal is then able to donate electron density from its d-character HOMO into the olefin's empty π^* LUMO, which is referred to as back-bonding. Although experimental determinations of metal–olefin bond energies are scarce and difficult to obtain, there is evidence that indicates that trends in stability and bond strengths of metal–olefin complexes cannot always be rationalized in the context of the DCD model.^{6–8} In some of these cases, it has been hypothesized⁶ that “steric effects” are the source of the observed

“anomalies”, but only a few studies address this issue from a quantitative perspective.^{7–11}

Density functional theory (DFT) calculations, which have become a reliable source of metal–ligand bond energies,^{12–14} provide an opportunity to obtain quantitative insights into metal–olefin interactions.¹⁵ As such, these calculations can be used to explain trends in BDEs, to test available models for bonding, and to attempt to formulate more quantitative models of bonding.

Experimental gas-phase Cr–olefin bond dissociation enthalpies (BDEs) are available for the Cr(CO)₅(C₂H₄)^{16,17} and Cr(CO)₅(C₂F₄)¹⁷ complexes. Interestingly, the Cr–C₂F₄ bond energy is slightly smaller than the Cr–C₂H₄ bond energy. However, in a homologous series of metal–olefin complexes, prevailing “conventional wisdom” (typically based on interpretations of the DCD model) indicates that more electron withdrawing substituents would, a priori, be expected to lead to stronger π interactions, which will favor a stronger metal–

(8) Tollman, C. A. *J. Am. Chem. Soc.* **1974**, *96*, 2780.

(9) Nunzi, F.; Sgamelotti, A.; Re, N.; Floriani, C. *J. Chem. Soc., Dalton Trans.* **1999**, 3487.

(10) White, D. P.; Brown, T. L. *Inorg. Chem.* **1995**, *34*, 2718.

(11) Desmarais, N. D.; Adamo, C.; Panunzi, B.; Barone, V.; Giovannitti, B. *Inorg. Chim. Acta* **1995**, *238*, 159.

(12) (a) Ziegler, T. *Chem. Rev.* **1991**, *91*, 651. (b) Ziegler, T. *Can. J. Chem.* **1995**, *73*, 743.

(13) Frenking, G.; Antes, I.; Böhme, M.; Dapprich, S.; Ehlers, A. W.; Jonas, V.; Neuhaus, A.; Otto, M.; Stegman, R.; Veldkamp, A.; Vydroshchikov, S. F. In *Reviews in Computational Chemistry*; Lipkowitz, K. B., Boyd, D. B., Eds.; VCH: New York, 1996; Vol. 8.

(14) Laird, B. B.; Ross, R. B.; Ziegler, T. In *Chemical Applications of Density Functional Theory*; Laird, B. B., Ross, R. B., Ziegler, T., Eds.; ACS Symposium Series 629; American Chemical Society: Washington, DC, 1996; Chapter 1.

(15) Frenking, G.; Pidun, U. *J. Chem. Soc., Dalton Trans.* **1997**, 1653.

(16) (a) McNamara, B.; Becher, D. M.; Towns, M. H.; Grant, E. R. *J. Phys. Chem.* **1994**, *98*, 4622. (b) McNamara, B.; Towns, M. H.; Grant, E. R. *J. Am. Chem. Soc.* **1995**, *117*, 12254.

(17) Wells, J. R.; House, P. G.; Weitz, E. *J. Phys. Chem.* **1994**, *98*, 11256.

[†] Current address: Department of Chemistry, Illinois State University, Normal IL 61790.

(1) Collman, J. P.; Hegedus, L. S.; Norton, J. R.; Finke, R. G. *Principles and Applications of Organotransition Chemistry*; University Science Books: Mill Valley, CA, 1987.

(2) Crabtree, R. H. *The Organometallic Chemistry of the Transition Metals*; Wiley: New York, 2001.

(3) Yamamoto, A. *Organotransition Metal Chemistry*; Wiley: New York, 1986.

(4) Dewar, M. J. S. *Bull. Chem. Soc. Fr.* **1951**, *18*, C79.

(5) Chatt, J.; Duncanson, L. A. *J. Chem. Soc.* **1953**, 2939.

(6) Pruchnick, F. P. *Organometallic Chemistry of the Transition Elements*; Plenum: New York, 1990; Chapter 6, p 343.

(7) Cramer, R. *J. Am. Chem. Soc.* **1967**, *89*, 4621.

ligand bond, provided that σ donation, as is usually assumed, is not significantly affected.^{6,18} This would imply that the Cr–C₂F₄ bond should be stronger than the Cr–C₂H₄ bond because C₂F₄ is a more electron withdrawing ligand. However, it should be recognized that in its original formulation, the DCD model focused on how the electron withdrawing capabilities of ligands affect the contributions of the σ bonding and back-bonding interactions to the chemical bond. Additionally, because the DCD model is qualitative, there can be different views of what would be expected for trends in a homologous series of complexes. Experimental observations and previous DFT calculations¹⁹ demonstrate that the strength of the metal–olefin bond does not parallel the electronegativity of the substituent on the bound olefin in the series Cr(CO)₅(C₂X₄) (X = H, F, Cl). Prior DFT calculations for Cr(CO)₅(C₂Cl₄)¹⁹ predicted a dramatic decrease in the BDE of the Cr–C₂Cl₄ bond relative to the Cr–C₂H₄ bond. In fact, this theoretical result motivated the current experimental determination of the Cr–C₂Cl₄ BDE in Cr(CO)₅(C₂Cl₄) as well as further theoretical work on the factors behind the observed trend in BDEs in the Cr(CO)₅(C₂X₄) (X = H, F, Cl) series.

In this paper, we report the results of an experimental determination of the BDE of Cr(CO)₅(C₂Cl₄) and the results of DFT calculations. The experimental data provide a crucial additional data point for BDEs in the homologous series of complexes Cr(CO)₅(C₂X₄) (X = H, F, Cl). The DFT calculations are then used to explain the trends in the metal–olefin bond energies in this series in the context of a metal–olefin bond energy decomposition analysis (BEDA).²⁰ The analysis is used to quantify the σ and π electronic interactions between the olefin and Cr(CO)₅. The results are then discussed in the context of the DCD model. The analysis demonstrates that the deformation energy (i.e., the energy required to bring the olefin and Cr(CO)₅ to the geometry they adopt in the complex from the geometries of the isolated ground state species) can substantially alter predictions of bond strengths that are based solely on the electronic interactions and that the deformation energy can be the dominant factor in trends in BDEs in a homologous series of metal–olefin complexes.

II. Experimental Section

The experimental apparatus and methodology have been described in detail elsewhere.²¹ A brief description is given here for convenience. Gas-phase Cr(CO)₆ (~0.05 Torr), CO (1–10 Torr), C₂Cl₄ (0.2–5.0 Torr), and enough He (>35 Torr) to ensure that ligand association reactions take place in the high-pressure limit (as judged by the fact that, below 35 Torr He, the measured rates were invariant when higher pressures of He were used) were introduced into a 42 cm water-jacketed Pyrex cell terminated with CaF₂ windows. Cr(CO)₆ was photolyzed with the 308 nm output of a pulsed (1 Hz) excimer laser (Lambda Physik, LPX100) operating on XeCl, with a fluence of ~6–7 mJ/cm² at the cell window. A tunable IR diode laser (Laser Photonics) was used to probe the reactants, intermediates, and products in the CO stretching region (1950–2090 cm⁻¹) of the spectrum as a function of C₂Cl₄ and CO pressures. The intensity of the infrared probe laser was monitored with a fast response (250 ns) liquid N₂-cooled detector (Judson). The signal was amplified ($\times 100$, Perry) and fed to a digital oscilloscope (Lecroy 9400), and the average of at least 10 laser pulses was sent to a computer for analysis. Temperature control was achieved using a constant-temperature bath, which circulated water through the

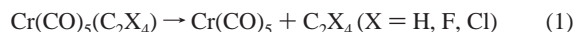
cell jacket. The temperature was monitored by a chromel–alumel thermocouple and was varied over the range 288–308 K with an uncertainty of ± 1 K.

Cr(CO)₆ (Strem Chemicals) and C₂Cl₄ (99.9% Aldrich) were subjected to at least three freeze–thaw–pump cycles prior to use. CO (99.9%, Matheson) and helium (99.999%, Matheson) were used as received.

III. Computational Method

Equilibrium geometries were calculated with the Jaguar quantum chemistry program.²² All the calculations were performed using density functional theory (DFT) with the local density approximation (LDA) of Vosko, Wilk, and Nusair (VWN).²³ In addition, nonlocal density functionals were added self-consistently. Becke's²⁴ was used for exchange, and Perdew's,²⁵ for correlation (BP86). Hay and Wadt's effective core potential (ECP)²⁶ basis set was used for chromium, and the 6-311G** basis set²⁷ was used for nonmetal atoms. The frozen core approximation was used, in which the outermost core orbitals were included.

Bond energies (ΔE) were calculated from the difference in the optimized energies of the ground states of the products and the reactants for the reaction:



$$\Delta E = E[\text{Cr(CO)}_5] + E[\text{C}_2\text{X}_4] - E[\text{Cr(CO)}_5(\text{C}_2\text{X}_4)] \quad (2)$$

This energy, ΔE , represents the reaction energy for olefin dissociation. Thus, by this definition, *factors that lead to an increase in bonding interactions are positive; those that lead to a decrease are negative.*

Bond enthalpies at 298 K are calculated from ΔE according to the expression²⁸

$$\Delta H_{\text{calc}} = \Delta E + \Delta \text{ZPE} + \Delta E_{\text{th}} + \Delta(PV) \quad (3)$$

where ΔZPE is the zero point energy correction obtained from a calculation of the vibrational frequencies, ΔE_{th} is the change associated with the translational, rotational, and vibrational energy in going from 0 to 298 K, and $\Delta(PV)$ is the molar work, which is equal to ΔnRT . The basis set superposition error (BSSE) correction was not included because it decreases the calculated enthalpy values to a point where they are significantly below the experimental values. However, inclusion of the BSSE does not change the trend in the calculated bond enthalpies. This is discussed in more detail in ref 29.

Bond energy decomposition analyses (BEDA)²⁰ were performed using the Amsterdam Density Functional program (ADF2000)³⁰ with the same DFT functional (VWN/BP86) used for energy minimization. However, when using ADF, the atomic orbitals on chromium were described by an uncontracted triple- ζ STO basis set,³¹ while a double- ζ STO basis set was used for nonmetal atoms. A single- ζ polarization

(22) Jaguar 4.0; Schrödinger Inc.: Portland, OR, 1998–1999.

(23) Vosko, S. H.; Wilk, L.; Nusair, M. *Can. J. Phys.* **1980**, *58*, 1200.

(24) Becke, A. D. *Phys. Rev. A* **1988**, *38*, 3098.

(25) (a) Perdew, J. P. *Phys. Rev. B* **1986**, *33*, 8822. (b) Perdew, J. P. *Phys. Rev. B* **1986**, *34*, 7406.

(26) Hay, P. J.; Wadt, W. R. *J. Chem. Phys.* **1985**, *82*, 299.

(27) (a) Clark, T.; Chandrasekhar, J.; Spitznagel, G. W.; Schleyer, P. v. R. *J. Comput. Chem.* **1983**, *4*, 294. (b) Frisch, M. J.; Pople, J. A.; Binkley, J. S. *J. Chem. Phys.* **1984**, *80*, 3265. (c) Krishnan, R.; Binkley, J. S.; Seeger, R.; Pople, J. A. *J. Chem. Phys.* **1980**, *72*, 650. (d) McLean, A. D.; Chandler, G. S. *J. Chem. Phys.* **1980**, *72*, 5639.

(28) Deakyn, C. A.; Liebman, J. F. In *Encyclopedia of Computational Chemistry*; Schleyer, P. v. R., Allinger, N. R., Clark, T., Gasteiger, J., Kollman, P. A., Schaefer, H. F., III, Schreiner, P. R., Eds.; Wiley: Chichester, U.K., 1998; Vol. 2, p 1439.

(29) Cedeño, D. L.; Weitz, E.; Bérces, A. *J. Phys. Chem. A* **2001**, *105*, 8077–8085.

(30) (a) *Amsterdam Density Functional*, ADF2000; SCM, Vrije Universiteit: The Netherlands. (b) Baerends, E. J.; Ellis, D. E.; Ros, P. *Chem. Phys.* **1973**, *2*, 41. (c) Versluis, L.; Ziegler, T. *J. Chem. Phys.* **1988**, *88*, 322. (d) te Velde, G.; Baerends, E. *J. Theor. Chem. Acc.* **1998**, *99*, 391. (e) Fonseca Guerra, C.; Snijders, J. G.; te Velde, G.; Baerends, E. *J. Theor. Chem. Acc.* **1998**, *99*, 391.

(18) Ref 2, Chapter 5, p 116.

(19) Wang, W.; Weitz, E. Unpublished results using *Gaussian 94* and a PZ91/BP86 functional.

(20) (a) Ziegler, T.; Rauk, A. *Theor. Chim. Acta* **1977**, *46*, 1. (b) Ziegler, T.; Rauk, A. *Inorg. Chem.* **1979**, *18*, 1588. (c) Ziegler, T.; Rauk, A. *Inorg. Chem.* **1979**, *18*, 1755.

(21) Weitz, E. *J. Phys. Chem.* **1994**, *98*, 11256.

function and the frozen core approximation^{30b} were used for all atoms (except hydrogen). A set of auxiliary s, p, d, f, g, and h STO functions, centered on all nuclei, was used to fit the molecular density and represent the Coulomb and exchange potentials accurately in each SCF cycle.³²

In terms of the BEDA, the calculated bond energy (ΔE) is initially decomposed into two terms:

$$\Delta E = \Delta E_{\text{int}} + \Delta E_{\text{def}} \quad (4)$$

The first term in eq 4 (ΔE_{int}) is the energy due to the electronic bonding interactions between the olefin and $\text{Cr}(\text{CO})_5$. Because we take interactions that lead to an increase in the metal–olefin bond strength as being positive, ΔE_{int} is the energy required to break the bond yielding the olefin and $\text{Cr}(\text{CO})_5$ in a state in which their geometries are those that they have in the bound complex. This quantity is sometimes referred to as the “bond-snap” energy.⁹ ΔE_{int} can be further broken down into energy components for both the attractive and the repulsive electronic interactions of the molecular orbitals involved in the metal–olefin bond:

$$\Delta E_{\text{int}} = \Delta E_{\text{oi}} + \Delta E_{\text{elst}} + \Delta E_{\text{pauli}} \quad (5)$$

ΔE_{oi} is the attractive energy due to the interactions between occupied orbitals of one fragment and empty orbitals of the other fragment as well as between the occupied and empty orbitals within a given fragment (polarization). ΔE_{oi} can be further partitioned into a sum that contains a term for each irreducible representation of the interacting orbitals. ΔE_{elst} is the term due to the electrostatic interaction between the fragments, which, for neutral fragments, is normally attractive. ΔE_{pauli} is the Pauli repulsion energy term. The magnitude of the second term in eq 4 (ΔE_{def}) represents the energy required to deform the fragments from the geometries they have as isolated ground-state entities to the geometries they possess in the complex. By convention, this is a negative number. ΔE_{def} can be further decomposed into the contribution that results from the deformation of the olefin ($\Delta E_{\text{def}}(\text{olefin})$) and the contribution from the deformation of $\text{Cr}(\text{CO})_5$ ($\Delta E_{\text{def}}(\text{Cr}(\text{CO})_5)$).

IV. Results

A. Experimental Determination of Cr–C₂Cl₄ BDE. Time-resolved IR spectra of $\text{Cr}(\text{CO})_5(\text{C}_2\text{Cl}_4)$, in the CO stretching region, are shown in Figure 1. Two new absorption bands, at ~ 2030 and 2019 cm^{-1} , are observed when photolysis of $\text{Cr}(\text{CO})_6$ is performed with both C_2Cl_4 and CO present in the reaction mix. Both of these bands evolve in time at the same rate, as expected for two bands that belong to a single product. Because photolysis of $\text{Cr}(\text{CO})_6$ at 308 nm yields a mixture of $\text{Cr}(\text{CO})_4$ and $\text{Cr}(\text{CO})_5$,³³ the bands could, in principle, be due to the monoolefin and/or the bisolefin adducts. However, the fact that these bands are not observed in the absence of CO mitigates against their assignment to $\text{Cr}(\text{CO})_4(\text{C}_2\text{Cl}_4)_2$. The addition of CO and buffer gas optimizes the yield of $\text{Cr}(\text{CO})_5$ (monitored at 1979 cm^{-1}) and decreases the amount of $\text{Cr}(\text{CO})_4$ in the cell and, thus, the probability of forming the bisolefin product(s). The formation of a C_2Cl_4 adduct is monitored by observing the decay of $\text{Cr}(\text{CO})_5$ in the presence of C_2Cl_4 . The rate of decay of $\text{Cr}(\text{CO})_5$ is linearly dependent on the C_2Cl_4 pressure: thus, $\text{Cr}(\text{CO})_5$ adds C_2Cl_4 to form $\text{Cr}(\text{CO})_5(\text{C}_2\text{Cl}_4)$. The bimolecular rate constant for addition of C_2Cl_4 to $\text{Cr}(\text{CO})_5$ (k_L) was obtained from the slope of the plot for the rate of decay of $\text{Cr}(\text{CO})_5$ versus the C_2Cl_4 pressure. It has a value of $(2.8 \pm 0.5) \times 10^{-11} \text{ cm}^3 \text{ molecule}^{-1} \text{ s}^{-1}$ at 297 K and is temperature

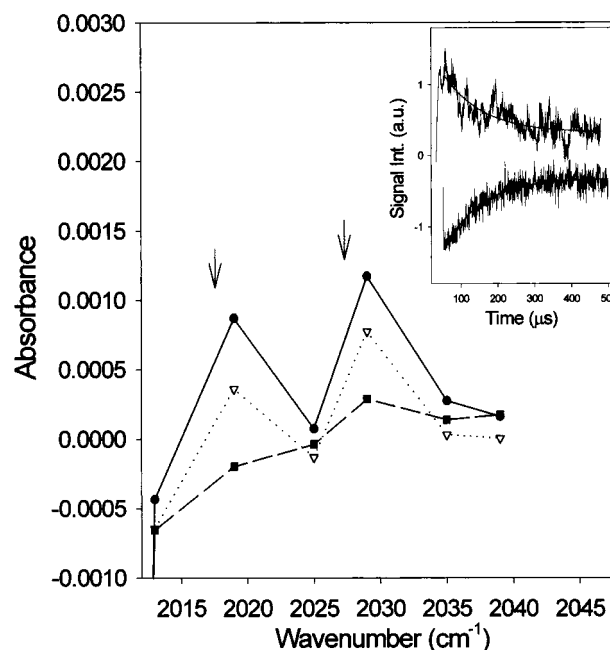


Figure 1. Transient IR spectra of $\text{Cr}(\text{CO})_5(\text{C}_2\text{Cl}_4)$. The spectra were taken 100 (●), 200 (▽), and 375 (■) μs after photolysis. Arrows indicate the direction of evolution of the traces. The top trace in the insert is the decay ($t_{1/2} = 73 \pm 7 \mu\text{s}$) of $\text{Cr}(\text{CO})_5(\text{C}_2\text{Cl}_4)$ at 2030 cm^{-1} ; the bottom trace is the recovery ($t_{1/2} = 68 \pm 4 \mu\text{s}$) of $\text{Cr}(\text{CO})_6$ at 2001 cm^{-1} for a $\text{C}_2\text{Cl}_4/\text{CO}$ pressure ratio of 2.5. The solid lines drawn through these traces are the fits.

Table 1. Cr–Olefin Bond Energetics and CO Stretching Frequencies for the $\text{Cr}(\text{CO})_5(\text{C}_2\text{X}_4)$ Complexes^a

	H	F	Cl
ΔH_{298}	24.8 ± 1.2^b	19.7 ± 1.4^c	12.8 ± 1.6^d
ΔH_{calc}	22.8	18.1	10.8
ΔE	26.6	20.2	11.4
χ (Pauling) ^e	2.20	3.98	3.16
ν_{CO} (cm^{-1})	1975 ^f	2018 ^c	2019 ^d
	1980	2030	2030

^a Energies in kcal/mol, frequencies in cm^{-1} . ^b Average value from refs 16 and 17. ^c From ref 17. ^d This work. ^e Electronegativity from ref 56. ^f From ref 16b.

independent, within experimental error, over the relevant temperature range. This value for k_L is comparable to the reported values for the rate constant for the association processes of $\text{Cr}(\text{CO})_5$ and other ligands.¹⁷ Additional evidence for the assignment of the observed bands to $\text{Cr}(\text{CO})_5(\text{C}_2\text{Cl}_4)$ comes from the fact that the experimental frequencies are very similar to those previously reported for $\text{Cr}(\text{CO})_5(\text{C}_2\text{F}_4)$ ¹⁷ (see Table 1). DFT calculations also indicate that the unscaled CO stretching frequencies of both $\text{Cr}(\text{CO})_5(\text{C}_2\text{F}_4)$ (2002, 1999 cm^{-1}) and $\text{Cr}(\text{CO})_5(\text{C}_2\text{Cl}_4)$ (2004, 1999 cm^{-1}) should be very similar. Consistent with our assignment, and as shown in eqs 6–8, when $\text{Cr}(\text{CO})_5(\text{C}_2\text{Cl}_4)$ loses C_2Cl_4 and adds CO, $\text{Cr}(\text{CO})_6$ is regenerated. To our knowledge, this is the first time $\text{Cr}(\text{CO})_5(\text{C}_2\text{Cl}_4)$ has been detected. As seen in Table 1, the CO stretching frequencies for metal complexes of halogenated olefins are shifted to higher energy relative to those of $\text{Cr}(\text{CO})_5(\text{C}_2\text{H}_4)$.

The unimolecular rate constant for dissociative loss of C_2Cl_4 (k_d) can be determined from the following kinetic scheme (eqs 6–8) by application of the steady-state approximation to $\text{Cr}(\text{CO})_5$ to give the result in eq 9.²¹ In eq 9, k_{obs} is the experimentally observed rate of regeneration of parent (or equivalently the rate of loss of $\text{Cr}(\text{CO})_5(\text{C}_2\text{Cl}_4)$).

(31) (a) Snijders, G. J.; Baerends, E. J.; Vernooijs, P. *At. Data Nucl. Data Tables* **1982**, 26, 483. (b) Vernooijs, P.; Snijders, G. J.; Baerends, E. J. *Slater Type Basis Functions for the Whole Periodic System*; Internal Report; Free University of Amsterdam: The Netherlands, 1981.

(32) Krijn, J.; Baerends, E. J. *Fit functions in the HFS-method*; Internal Report; Free University of Amsterdam: The Netherlands, 1984.

(33) Ishikawa, Y.; Brown, C. E.; Hackett, P. A.; Rayner, D. M. *J. Phys. Chem.* **1990**, 94, 2404.



$$k_{\text{obs}} = \frac{k_d k_{\text{CO}} [\text{CO}]}{k_{\text{CO}} [\text{CO}] + k_L [\text{L}]} \quad (9)$$

This mechanism is predicated on dissociative loss of C_2Cl_4 . Dissociative loss of weakly bound ligands is expected, especially when “ligand slippage” processes, which can open up a site in the coordination sphere of the metal, are effectively precluded. Without ligand slippage, an associative substitution process would require a greater than 18 electron intermediate. This is an unlikely occurrence in this system, because the relevant ligand association processes are unactivated. Additionally, a wide variety of $\text{Cr}(\text{CO})_5(\text{olefin})$ complexes undergo dissociative loss of the olefin.^{16,17,21} However, the most compelling evidence for a dissociative loss process is that the variation of the observed values for k_{obs} are consistent with eq 9. When this equation is rewritten in the following form,

$$\frac{1}{k_{\text{obs}}} = \frac{1}{k_d} + \frac{k_L}{k_d k_{\text{CO}}} \frac{[\text{C}_2\text{Cl}_4]}{[\text{CO}]} \quad (10)$$

it becomes apparent that k_{obs} should depend on the $\text{C}_2\text{Cl}_4/\text{CO}$ pressure ratio rather than the individual pressures. The recovery rate of the $\text{Cr}(\text{CO})_6$ was monitored at 2001 cm^{-1} for different $\text{C}_2\text{Cl}_4/\text{CO}$ pressure ratios, and the expected dependence was observed (see Figure 2). In addition, in a few cases, common $\text{C}_2\text{Cl}_4/\text{CO}$ pressure ratios were obtained by varying the individual ligand pressures. As expected, k_{obs} depended on the pressure ratio, not the individual pressures.

The value of k_d can then be obtained directly from eq 9, if the rate constants for ligand addition (k_L and k_{CO}) are known. There are prior determinations of k_{CO} , which center around two different values.^{17,33–38} The intercepts of the C_2Cl_4 dependent rate data are all consistent with the value of $(2.5 \pm 0.5) \times 10^{-11} \text{ cm}^3 \text{ molecule}^{-1} \text{ s}^{-1}$ for k_{CO} .³⁴ Thus, this value has been used in the present work. This rate constant has been determined to be temperature independent, within experimental error, over the relevant temperature range.

An Arrhenius analysis (see Figure 2) of k_d in the temperature range 288–308 K gives an activation energy for olefin dissociation of $12.2 \pm 1.6 \text{ kcal/mol}$ and a preexponential of $\ln A = 31.1 \pm 3.0$. The value for the preexponential is consistent with a value that would be expected for dissociation of a small olefin from a metal carbonyl.^{17,21} To our knowledge, all gas-phase reactions of small ligands with $\text{Cr}(\text{CO})_5$, in which the temperature dependence of the rate constant has been studied, have been reported to be unactivated.^{17,21} As expected, the rate constant for the association reaction to form $\text{Cr}(\text{CO})_5(\text{C}_2\text{Cl}_4)$ is unactivated within the experimental error limits and has a magnitude similar to that measured for association reactions of other small olefins with $\text{Cr}(\text{CO})_5$.¹⁷ Then, the BDE for this

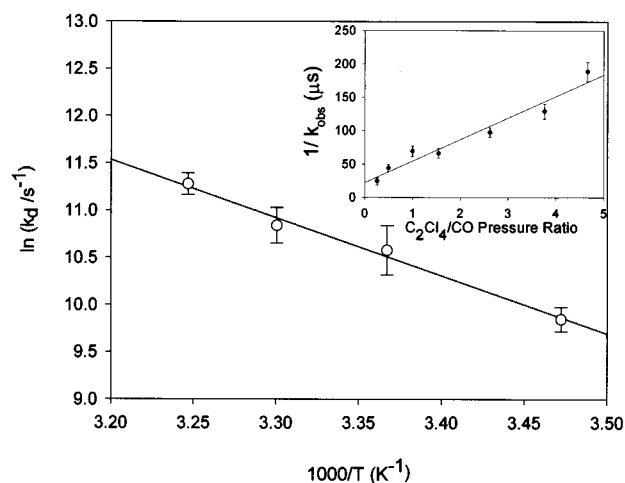


Figure 2. Arrhenius plot for the dissociation of $\text{Cr}(\text{CO})_5(\text{C}_2\text{Cl}_4)$ over the temperature range 288–308 K. The insert shows that the decay follows the behavior predicted by eq 10.

Table 2. Results of the Bond Energy Decomposition Analysis (kcal/mol) for the $\text{Cr}(\text{CO})_5(\text{C}_2\text{X}_4)$ Complexes

	H	F	Cl
ΔE_{oi}	56.3	92.0	75.6
ΔE_{A1}	30.6	37.5	26.8
ΔE_{A2}	0.7	1.1	1.4
ΔE_{B1^a}	2.6	7.3	7.0
ΔE_{B2^a}	22.4	46.1	40.4
ΔE_{elst}	74.1	86.2	86.6
ΔE_{pauli}	−97.5	−133.4	−128.5
$\Delta E_{\text{def}}(\text{olefin})$	−5.3	−22.2	−19.2
$\Delta E_{\text{def}}(\text{Cr}(\text{CO})_5)$	−1.0	−2.4	−3.1

^a The B_1 symmetry orbital has mainly d_{xz} character, and the B_2 symmetry orbital has mainly d_{yz} character.

complex can be calculated from the activation energy for the loss of C_2Cl_4 ($\Delta H = E_a + \Delta nRT$).^{17,21} This procedure gives $\Delta H = 12.8 \pm 1.6 \text{ kcal/mol}$ at 298 K. Table 1 also provides the experimental BDEs for $\text{Cr}(\text{CO})_5(\text{C}_2\text{H}_4)$ and $\text{Cr}(\text{CO})_5(\text{C}_2\text{F}_4)$. The measured bond enthalpy for the $\text{Cr}-\text{C}_2\text{Cl}_4$ bond in $\text{Cr}(\text{CO})_5(\text{C}_2\text{Cl}_4)$ is significantly smaller than the previously determined bond enthalpies for the metal–olefin bond in the analogous C_2H_4 and C_2Cl_4 complexes.

B. DFT Bond Energies and Geometries. Table 1 also shows calculated $\text{Cr}-\text{C}_2\text{X}_4$ bond energies (ΔE) and bond enthalpies (ΔH_{cal}) for $\text{Cr}(\text{CO})_5(\text{C}_2\text{X}_4)$ ($\text{X} = \text{H}, \text{F}, \text{Cl}$) based on eqs 2 and 3. The agreement between the experimental and calculated values for ΔH is good. Table 2 shows the results of the BEDA for these complexes based on eq 5. This table includes the energies resulting from decomposing ΔE_{oi} in terms of the irreducible representations ($\text{A}_1, \text{A}_2, \text{B}_1, \text{B}_2$) for the C_{2v} point group. ΔE_{oi} is dominated by contributions from the A_1 (σ -donation) and B_2 (back-bonding) symmetry frontier molecular orbitals (FMOs). However, there is a non-negligible contribution from the B_1 term that is a result of electron donation from the next lowest occupied orbital relative to the HOMO of the metal to the unoccupied orbital that is immediately above the LUMO of the olefin. This term is larger for the halogenated complexes than for the ethylene complex. The trend for ΔE_{oi} is $\text{C}_2\text{F}_4 > \text{C}_2\text{Cl}_4 > \text{C}_2\text{H}_4$, which follows the trend in the electronegativity of the substituent. The electrostatic term is an “attractive” term that is of similar magnitude for both halogenated complexes and is larger for these complexes than for the ethylene complex. The Pauli repulsion is larger than the electrostatic attraction for all the complexes, and the trend in the magnitude of this term

(34) Seder, T. A.; Church, S. P.; Weitz, E. *J. Am. Chem. Soc.* **1986**, *108*, 4721.

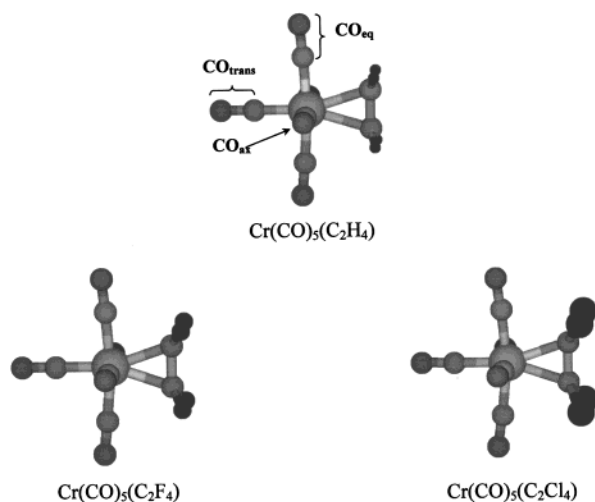
(35) Seder, T. A.; Church, S. P.; Ouderkerk, A. J.; Weitz, E. *J. Am. Chem. Soc.* **1985**, *107*, 1432.

(36) Fletcher, T. R.; Rosenfeld, R. N. *J. Am. Chem. Soc.* **1986**, *108*, 1686.

(37) Kelly, J. M.; Bent, D. V.; Hermann, H.; Schulte-Frohlinde, D.; Koerner von Gustorf, E. *J. Organomet. Chem.* **1974**, *69*, 259.

(38) Kelly, J. M.; Long, C.; Bonneau, R. *J. Phys. Chem.* **1983**, *87*, 3344.

Chart 1

Table 3. Calculated Geometries^a for the Cr(CO)₅(C₂X₄) Complexes

	H	F	Cl	exptl ^c
Cr–C _{olef}	2.327	2.202	2.280	2.393(4) ^d
Cr–C _{ax}	1.902	1.910	1.914	1.923(5) ^d
Cr–C _{eq}	1.899	1.907	1.912	1.888(5) ^d
Cr–C _{trans}	1.862	1.889	1.878	1.849(6)
C–O _{ax}	1.156	1.152	1.152	
C–O _{eq}	1.156	1.152	1.151	
C–O _{trans}	1.158	1.153	1.155	
C _{ax} –Cr–C _{ax}	179.9	180.2	184.1	180.7(2)
C _{eq} –Cr–C _{eq}	186.6	189.2	191.5	186.9(2)
Cr–C–O _{ax}	178.1	177.4	174.7	
Cr–C–O _{eq}	177.9	178.8	177.0	
Cr–C–O _{trans}	180.0	180.0	180.0	
C–C	1.385	1.414	1.425	1.363(6)
C–X	1.089	1.350	1.775	
X–C–X	116.0	110.6	110.8	
Θ ^b	20.9	39.2	36.9	

^a Bond lengths in Å, angles in deg. The subscript eq refers to the two COs positioned in the same plane as the C–C bond, ax refers to the two COs positioned in the plane perpendicular to the C–C plane, and trans refers to the CO trans to the olefin. ^b The pyramidalization angle (in deg) is defined as the difference between 180° and the X–C–C–X dihedral angle in the bound olefins (Θ = 0 for free olefins). ^c From ref 41. ^d Average value for Cr(CO)₅(endo-6-aryl bicyclo[3.1.0]hex-2-ene).

nearly parallels the trend in Δ*E*_{elst}. Finally, the total deformation energy is significantly larger for the halogenated complexes than for Cr(CO)₅(C₂H₄). A discussion of how the trends in the BEDA terms affect the trend in the BDE is presented in the next section.

Chart 1 shows the calculated geometries for the Cr(CO)₅(C₂X₄) complexes, and Table 3 summarizes the relevant geometrical data. Table 4 contains geometrical data for the ground state of the free olefins and for Cr(CO)₅. To our knowledge, there are no experimental data on the geometries of the Cr(CO)₅(C₂X₄) complexes under consideration. However, because the calculated geometrical data for the relevant iron complexes²⁹ correlated well with experimental data for Fe(CO)₄(C₂H₄)³⁹ and Fe(CO)₄(C₂F₄)⁴⁰, we expect similar reliability in the data in Table 3.

Furthermore, the experimental geometry for Cr(CO)₅(endo-6-aryl bicyclo[3.1.0]hex-2-ene)⁴¹ is known and is included in

(39) Davis, M. I.; Speed, C. S. *J. Organomet. Chem.* **1970**, *21*, 401.

(40) Beagley, B.; Schmidling, D. G.; Cruickshank, D. W. *J. Acta Crystallogr.* **1973**, *B29*, 1499.

(41) Fischer, H.; Hofmann, J. *Chem. Ber.* **1991**, *124*, 981.

Table 4. Calculated Geometries^a for the Ground State of Cr(CO)₅(C_{4v}) and Olefins (C₂X₄)

Cr(CO) ₅						
Cr–C _{cis}	Cr–C _{trans}	C–O _{cis}	C–O _{trans}	C _{cis} –Cr–C _{cis}	Cr–C–O _{cis}	Cr–C _{cis}
1.906	1.828	1.155	1.161	179.9	177.6	1.906
Free Olefins						
X	C–C	C–X	X–C–X			
H	1.334	1.091	116.5			
F	1.333	1.329	113.5			
Cl	1.355	1.742	115.4			

^a Bond lengths in Å, and angles in deg; subscript cis refers to the 4 COs positioned in the molecular plane containing the metal, and trans to the CO perpendicular to such plane, along the C₄ symmetry axis.

Table 3. The experimentally determined Cr–C_{olef} and Cr–C(O) bond lengths for the bicycloolefin complex and the calculated data for Cr(CO)₅(C₂H₄) agree well, suggesting that the calculated structures are reliable. This is also indicated by the fact that the trends for the experimental Cr–C(O) bond lengths within the bicycloolefin complex are reproduced by the calculations, that is, Cr–C_{trans} < Cr–C_{eq} < Cr–C_{ax}.

Clearly, as seen in Table 3, the Cr–C(O) and C–O bond lengths correlate well with the electron withdrawing capability of the olefin (electronegativity of the substituent), especially for the CO trans to the olefin. As expected, strongly electron withdrawing olefins such as C₂F₄ and C₂Cl₄ compete more effectively than C₂H₄ for electron density with the trans CO, making the Cr–C(O) bond more labile; thus, the longest Cr–C bond length is in the perfluoroethylene complex, which contains the most electronegative olefinic substituents (F). In addition, the CO trans to a strongly electron withdrawing olefin has less electron density to back-bond, which means that less electron density is being put into the π antibonding MO of CO. As a result, the bond length of the CO trans to halogenated olefins decreases relative to the bond length of a CO trans to C₂H₄.

V. Discussion

A. Cr–Olefin Bonding Interactions and Trends in BDEs.

The measured bond enthalpy for the Cr–C₂Cl₄ bond in Cr(CO)₅(C₂Cl₄) (12.8 ± 1.6 kcal/mol) is significantly smaller than the previously determined bond enthalpies for the metal–olefin bond in Cr(CO)₅(C₂H₄) (24.8 ± 1.2 kcal/mol)^{16,17} and in Cr(CO)₅(C₂F₄) (19.7 ± 1.4 kcal/mol).¹⁷ It is often assumed that more electron withdrawing substituents should lead to stronger π interactions, which in turn favor a stronger metal–ligand bond.^{4,6,18} However, as mentioned in the Introduction, the trend in BDEs for this series of complexes does not parallel the trend in electronegativities of the substituents on the olefin. The results of the BEDA help explain the trend in BDEs by providing a quantification of the metal–olefin bonding interactions and their effect on metal–olefin bond strengths.

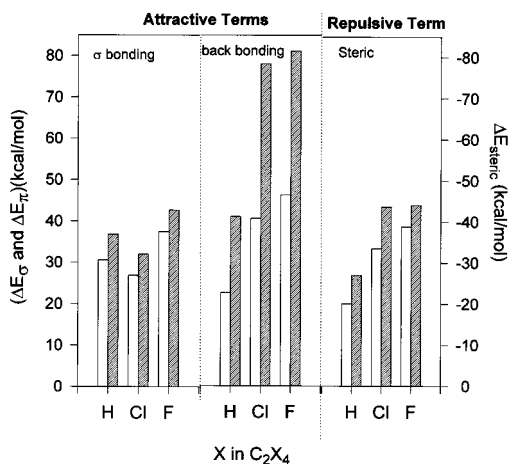
The DCD model is based on a frontier molecular orbital (FMO) picture of the metal–ligand σ and π interactions in a complex. The energy that characterizes these interactions can be written as

$$\Delta E_{\text{DCD}} = \Delta E_{\sigma} + \Delta E_{\pi} \quad (11)$$

Table 5 shows the calculated Δ*E*_{DCD} values for both Cr(CO)₅(C₂X₄) and Fe(CO)₄(C₂X₄) complexes. Because the attractive orbital interaction term (Δ*E*_{oi} in eq 5) can be decomposed into the irreducible representations of the interacting orbitals, it is possible to quantify the energy gained due to σ donation (Δ*E*_σ, the A₁ term in Table 2) and that due to the π interaction (Δ*E*_π,

Table 5. Calculated ΔE_{DCD} Values (in kcal/mol) for $\text{Cr}(\text{CO})_5(\text{C}_2\text{X}_4)$ and $\text{Fe}(\text{CO})_4(\text{C}_2\text{X}_4)$ Complexes

	$\text{Cr}(\text{CO})_5(\text{C}_2\text{X}_4)$	$\text{Fe}(\text{CO})_4(\text{C}_2\text{X}_4)$
H	53.0	77.6
F	83.6	123.5
Cl	67.2	109.7

**Figure 3.** Electronic interaction energies for $\text{Cr}(\text{CO})_5(\text{C}_2\text{X}_4)$ and $\text{Fe}(\text{CO})_4(\text{C}_2\text{X}_4)$ ($X = \text{H}, \text{F}, \text{Cl}$) complexes. The plot on the left side corresponds to σ -donation (ΔE_σ), the plot in the center to back-bonding (ΔE_π), and the plot on the right side to the repulsive term (ΔE_{steric}). White bars are for the chromium complexes, and patterned bars are for the iron complexes.

the B_2 term in Table 2). The electronic interaction energy (ΔE_{int} , eq 5) can be written as

$$\Delta E_{\text{int}} = \Delta E_\sigma + \Delta E_\pi + \Delta E_{A_2} + \Delta E_{B_1} + \Delta E_{\text{elst}} + \Delta E_{\text{Pauli}} \quad (12)$$

The term ΔE_{B_1} is responsible for a small but non-negligible fraction of the orbital interaction energy ΔE_{oi} . It originates from the interaction of orbitals that are not FMOs: the MO just below the metal HOMO and the MO just above the LUMO of the olefin. However, it should be noted that even if the DCD model were extended to include this term, the magnitude of ΔE_{B_1} is small compared to ΔE_σ and ΔE_π , and thus, its inclusion would not change the trend for the magnitude of ΔE_{DCD} .

Of the remaining terms in eq 12, the sum of $\Delta E_{\text{elst}} + \Delta E_{\text{Pauli}}$ is often called ΔE_{steric} .²⁰ ΔE_{elst} is an attractive (positive) term, while ΔE_{Pauli} is a repulsive (negative) term that dominates the sum, making ΔE_{steric} negative. We can then write that

$$\Delta E_{\text{int}} = \Delta E_{\text{DCD}} + \Delta E_{\text{steric}} + \Delta E_{A_2} + \Delta E_{B_1} \quad (13)$$

The calculated values for ΔE_{int} (the energy necessary to “snap” the metal–ligand bond while leaving the metal-centered species and olefin in the geometry they assume in the complex, i.e., the “bond-snap” energy) in the $\text{Cr}(\text{CO})_5(\text{C}_2\text{X}_4)$ complexes are 44.8, 33.7, and 32.9 kcal/mol for $X = \text{F}, \text{H}$, and Cl , respectively. Figure 3 shows the contribution of ΔE_σ , ΔE_π , and ΔE_{steric} to ΔE_{int} . The σ interaction for $\text{Cr}-\text{C}_2\text{F}_4$ is slightly larger (~ 7 kcal/mol) than the σ interaction in the $\text{Cr}-\text{C}_2\text{H}_4$ complex, but the dominant contribution to the attractive electronic interaction for the $\text{Cr}-\text{C}_2\text{F}_4$ complex originates from back-bonding.

Because of the superior electron withdrawing capability of fluorine relative to hydrogen, the back-bonding interaction for the $\text{Cr}-\text{C}_2\text{F}_4$ complex is, as expected, much larger (~ 24 kcal/mol) than the corresponding interaction in the $\text{Cr}-\text{C}_2\text{H}_4$ complex. On the basis of the electron withdrawing ability of

C_2Cl_4 relative to C_2H_4 , similar behavior was expected for the $\text{Cr}-\text{C}_2\text{Cl}_4$ interaction. However, ΔE_{int} for $\text{Cr}-\text{C}_2\text{Cl}_4$ is not significantly larger than ΔE_{int} for $\text{Cr}-\text{C}_2\text{H}_4$. The decomposition of ΔE_{int} in Figure 3 (on the basis of eq 13) shows that the energy due to σ donation for the C_2Cl_4 interaction with $\text{Cr}(\text{CO})_5$ decreases (~ 4 kcal/mol) relative to that of C_2H_4 , but this decrease is not enough to cancel the increase (~ 18 kcal/mol) in the back-bonding interaction energy of C_2Cl_4 relative to C_2H_4 . Further, Figure 3 demonstrates the importance of the repulsive term (ΔE_{steric}) in determining the magnitude of the “bond-snap” energies for the chromium complexes, and especially for the C_2Cl_4 complex relative to the C_2H_4 complex. The magnitude of ΔE_{steric} for $\text{Cr}(\text{CO})_5(\text{C}_2\text{Cl}_4)$ is large enough to effectively cancel a significant fraction of the energy that accrues from ΔE_{DCD} , resulting in a ΔE_{int} value for $\text{Cr}(\text{CO})_5(\text{C}_2\text{Cl}_4)$ that is similar to that for $\text{Cr}(\text{CO})_5(\text{C}_2\text{H}_4)$.

The repulsive Pauli electronic energy is larger in magnitude for the halogen complexes than for ethylene. This is a result of the steric interactions of the halogens with the CO ligands. However, the magnitude of this repulsive term depends on how close the olefin can get to the metal. Because each carbon in C_2F_4 is about 0.1 Å closer to chromium than the carbons in C_2Cl_4 , ΔE_{Pauli} is slightly larger for $(\text{CO})_5\text{Cr}(\text{C}_2\text{F}_4)$ than ΔE_{Pauli} for $(\text{CO})_5\text{Cr}(\text{C}_2\text{Cl}_4)$, although C_2Cl_4 is bulkier than C_2F_4 .

Insights into the effect of the central metal on the bonding interaction can be obtained from a comparison of the terms in the decomposition analysis in eq 13 for chromium versus iron carbonyl–olefin complexes.²⁹ The ΔE_σ , ΔE_π , and ΔE_{steric} values for both series of complexes are compared in Figure 3. Calculated values for ΔE_{int} for $(\text{CO})_4\text{Fe}-\text{C}_2\text{X}_4$ are larger than those for the corresponding chromium complexes. They are 77.4, 64.4, and 50.2 kcal/mol, for $X = \text{F}, \text{Cl}$, and H , respectively. Iron–olefin electronic interactions are stronger than corresponding bonding interactions in the chromium–olefin complexes, mostly as a result of an increase in back-bonding. This trend in ΔE_{int} is consistent with the qualitative expectations that a more basic metal, such as iron, should have a larger back-bonding interaction than a metal that is relatively more electron deficient, such as chromium. It is interesting to note that for both metals there is a clear trend for ΔE_{DCD} (see Table 5 and Figure 3). The magnitude of this term increases in parallel with the electronegativity of the substituent on the olefin ($\text{C}_2\text{F}_4 > \text{C}_2\text{Cl}_4 > \text{C}_2\text{H}_4$). Also, as Figure 3 demonstrates, with $\text{Cr}(\text{CO})_5(\text{C}_2\text{H}_4)$ being the only exception, the overall bonding interaction of the FMOs ($\Delta E_{\text{DCD}} = \Delta E_\sigma + \Delta E_\pi$) is dominated by back-bonding.

However, ΔE_{int} values are significantly larger than the actual BDEs. For instance, the $\text{Cr}-\text{C}_2\text{Cl}_4$ BDE is about half the $\text{Cr}-\text{C}_2\text{H}_4$ BDE, despite the fact that their electronic interaction energies (ΔE_{int}) are similar. Figure 4 presents the terms in eq 4 (ΔE , ΔE_{int} , and ΔE_{def}) in the form of a bar graph. From this graph, it is clear that, rather than the magnitude of the “bond-snap” energy (ΔE_{int}), the deformation energy of the complexes is the determining factor in the trend in the metal–olefin bond strengths in the chromium carbonyl–olefin complexes. The possibility that deformation energies could have a significant effect on bond energies has been recognized by a number of authors.^{9,29,42–48} Calculations by Cedeño et al.²⁹ and Nunzi et al.⁹ for other metal–olefin complexes have also shown that the deformation energy can be a dominant factor in determining the magnitude of a metal–olefin BDE. Beauchamp and Simões⁴³ have also made arguments, supported by Hückel calculations,

(42) Marks, T. J. In *Bonding Energetics in Organometallic Compounds*; ACS Symposium Series 428; Marks, T. J., Ed.; American Chemical Society: Washington, DC, 1990; Chapter 1.

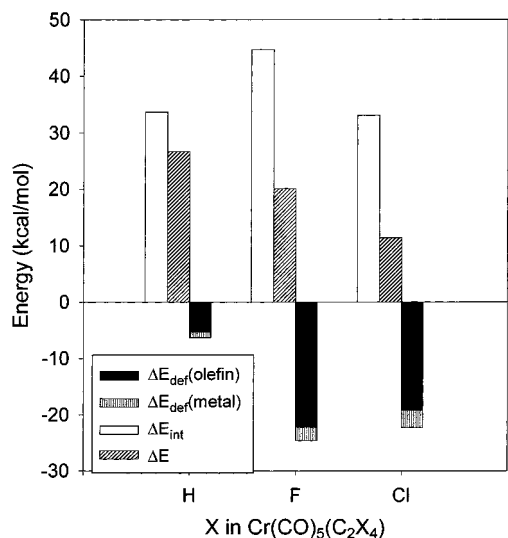


Figure 4. Energy decomposition analysis for $\text{Cr}(\text{CO})_5(\text{C}_2\text{X}_4)$. $\Delta E_{\text{def}}(\text{olefin})$ is the calculated olefin deformation energy, $\Delta E_{\text{def}}(\text{metal})$ is the calculated metal fragment deformation energy, ΔE_{int} is the calculated net electronic orbital bonding interaction energy, and ΔE is the calculated metal–olefin bond energy that results from the sum of ΔE_{int} and ΔE_{def} .

that the nature of the ligand and the metal can affect the deformation energies in $\text{M}(\text{Cp})_2\text{L}_2$ ($\text{M} = \text{Ti}, \text{W}$) complexes. They also point out that calculations of BDEs based on tabulated thermochemical data can lead to erroneous results unless deformation energies are explicitly considered.

B. Source of the Deformations. As seen in Figure 4, the magnitude of the total deformation energy for the $\text{Cr}(\text{CO})_5$ –olefin complexes increases in the order $\text{C}_2\text{H}_4 \ll \text{C}_2\text{Cl}_4 < \text{C}_2\text{F}_4$. Further insights into ΔE_{def} are obtained by partitioning this energy into contributions from the deformations of the olefin ($\Delta E_{\text{def}}(\text{olefin})$) and $\text{Cr}(\text{CO})_5$ ($\Delta E_{\text{def}}(\text{Cr}(\text{CO})_5)$). Values for these terms are given in Table 2. The magnitude of $\Delta E_{\text{def}}(\text{Cr}(\text{CO})_5)$ in the $\text{Cr}(\text{CO})_5(\text{C}_2\text{X}_4)$ complexes increases in the order $\text{C}_2\text{H}_4 < \text{C}_2\text{F}_4 < \text{C}_2\text{Cl}_4$. Geometrical changes in the $\text{Cr}(\text{CO})_5$ moiety correlate with the fragment deformation energy, particularly the bending of the CO ligands that are cis to the olefin (CO_{ax} and CO_{eq}). For both the equatorial and axial COs, the C–Cr–C and Cr–C–O angles increase (i.e., COs bend away from the olefin) as the size of the substituent increases. The equatorial COs experience larger repulsive forces than the axial ones, as evidenced by their larger C–Cr–C bending angle ($>6^\circ$) relative to the bending of the axial COs. This occurs because the equatorial COs are closer than the axial COs to the olefin substituents. The bending of the COs indicates that the deformation of $\text{Cr}(\text{CO})_5$ is a result of repulsive interactions similar to what has been seen for the analogous iron carbonyl–olefin complexes,²⁹ where there is a linear correlation between the bending angle of the COs and the van der Waals radii of the substituents on the olefin.

However, the overall ΔE_{def} for the complex is dominated by the deformation energy of the olefin ($\Delta E_{\text{def}}(\text{olefin})$). The

Table 6. Mulliken Populations (P) for the HOMO and LUMO of the Bound Olefins (C_2X_4)

X	$P(\text{HOMO})$	$P(\text{LUMO})$
H	1.63	0.28
F	1.62	0.47
Cl	1.75	0.44

geometry of the olefins changes significantly on bonding (see Tables 3 and 4). It is widely recognized that the olefinic carbon atoms rehybridize from sp^2 toward an sp^3 -like hybridization upon bonding to metal centers, as a consequence of the changes in the population (see Table 6) of the π and π^* frontier molecular orbitals.⁴⁹ As a result of this rehybridization, the C=C and C–X bonds elongate (with the exception of the C–H bond in C_2H_4 , whose C–H bond length is not very sensitive to whether the carbon is sp^2 or sp^3 hybridized), and the olefins deform from their planar geometry (measured from the pyramidalization angle (Θ) between the olefin substituents and the plane containing the C=C bond). The elongation of the C=C bond and the deviation from planarity are both larger for the halogenated olefins than for ethylene, increasing in proportion to the electronegativity of the substituent. An increase in the electronegativity of the substituent results in an increase in the electron withdrawing capability of the olefin that leads to greater back-bonding. The more electron density there is in the π^* LUMO, the greater is the sp^2 to sp^3 rehybridization of the olefin, causing a larger deformation that involves a higher associated energy cost. Although an increase in back-donation from the metal to the olefin leads to a strong metal–olefin interaction, the energy cost inherent in the deformation associated with the resulting rehybridization effectively cancels some of the increase in metal–olefin bond strength. These results are consistent with previous studies^{8,50–52} on strained cycloolefins that show that the metal–olefin bond strength increases with an increase in the strain in the cycloolefins. The likely explanation is that upon binding the strained olefins under study have to deform less than the unstrained olefins.

C. Correlation between Metal–Olefin Bond Lengths and Bond Strengths. For the complexes under study, DFT calculations can be used to assess the validity of the often assumed correlation between bond lengths and bond strengths.⁵³ Though DFT calculations often predict bond lengths that are somewhat longer than those determined from experiment,^{9,29} the experimentally determined bond lengths, which are available for $\text{Fe}(\text{CO})_4(\text{C}_2\text{H}_4)$ ³⁹ and $\text{Fe}(\text{CO})_4(\text{C}_2\text{F}_4)$,⁴⁰ provide a check on the accuracy of bond lengths calculated via DFT. In these systems, the calculated bond lengths exceed the experimentally determined lengths by ~ 0.03 Å, but the trends in calculated and experimental bond lengths agree. On the basis of these data and other calculations,^{9,15,26} we conclude that trends in bond lengths in the systems under study, calculated by DFT, can be expected to provide a good match with experimental trends.

In terms of the bond energy–bond order (BEBO) formalism, it would be expected to find a correlation between the Cr–olefin bond energies and bond lengths. Such a correlation is not observed for the calculated Cr–olefin bond enthalpies and bond lengths in the ethylene complex in comparison with the

(43) Martinho Simões, J. A.; Beauchamp, J. L. *Chem. Rev.* **1990**, *90*, 269.

(44) Comba, P. *Coord. Chem. Rev.* **1993**, *123*, 1.

(45) (a) Michalak, A.; Ziegler, T. *Organometallics* **2000**, *19*, 1850. (b) Margl, P.; Deng, L.; Ziegler, T. *J. Am. Chem. Soc.* **1998**, *120*, 5517.

(46) Cui, Q.; Musaev, D. G.; Morokuma, K. *Organometallics* **1997**, *16*, 1355.

(47) Dietz, M. L.; Bond, A. H.; Hay, B. P.; Chiarizia, R.; Huber, V. J.; Herlinger, A. W. *Chem. Commun.* **1999**, 1177.

(48) Pilcher, G. *Pure Appl. Chem.* **1989**, *61*, 855.

(49) See: (a) ref 1, p 150; (b) ref 2, p 107; (c) ref 3, p 220; (d) ref 6, p 329.

(50) Uddin, J.; Dapprich, S.; Frenking, G.; Yates, B. F. *Organometallics*, **1999**, *18*, 457.

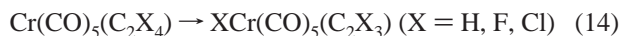
(51) Haddon, R. C. *J. Comput. Chem.* **1998**, *19*, 139.

(52) Klassen, J. K.; Yang, G. K. *Organometallics*, **1990**, *9*, 874.

(53) Johnston, H. S. *Gas-Phase Reaction Rate Theory*; Ronald Press: New York, 1966.

halogenated olefin complexes (Table 3). A similar lack of a bond length–bond energy correlation for the metal–C₂H₄ bond was found for the homologous series of complexes Fe(CO)₄–(C₂X₄) (X = H, F, Cl, Br, I).²⁹ Frenking and Pidun¹⁵ also obtained results in which the metal–olefin bond lengths and strengths for the W(CO)₅(C₂H₄) and the W(Cl)₄(C₂H₄) complexes do not correlate. These authors cautioned that “a distinction has to be made between metal–ligand interactions, as expressed by the bond length or distortion of the fragments and the bond dissociation energy”. Our conclusion is in agreement with theirs, indicating that the metal–olefin bond length is likely to correlate with the strength of the electronic interaction (ΔE_{int}) but not necessarily with the bond dissociation energy (ΔE). Therefore, as demonstrated here for the Cr(CO)₅–(C₂X₄) complexes, care should be exercised in inferring information about bond energies from bond lengths.

D. Change in Olefin Hybridization and Activation of the C–X Bond. Our experimental results indicate that Cr(CO)₅–(C₂Cl₄) decays via dissociative loss of olefin, as does Cr(CO)₅–(C₂H₄),^{16,17} Cr(CO)₅(C₂F₄),¹⁷ and other chromium pentacarbonyl–olefin complexes.^{16b} A dissociative olefin loss pathway is also observed for Fe(CO)₄(C₂H₄)⁵⁴ and Fe(CO)₄(C₂F₄).^{54b} In contrast, the lowest energy channel for the decay of Fe(CO)₄(C₂Cl₄) is an intramolecular oxidative addition process that yields ClFe(CO)₄(C₂Cl₃) by C–Cl bond activation.⁵⁵ Interestingly, C–Cl activation of C₂Cl₄ is observed when it is bound to Fe(CO)₄ but not when it is bound to Cr(CO)₅. To gain insights into the source of this switch in reaction pathways, the energy changes (ΔE_{rxn}) associated with the intramolecular oxidative addition reaction of olefins bound to chromium (eq 14) were calculated and compared to those previously calculated for iron.²⁹



$$\Delta E_{\text{rxn}} = E[\text{XCr}(\text{CO})_5(\text{C}_2\text{X}_3)] - E[\text{Cr}(\text{CO})_5(\text{C}_2\text{X}_4)] \quad (15)$$

The results are shown in Figure 5. The ΔE_{rxn} values for all the chromium complexes are positive. This implies that in all cases the reaction is endoenergetic, which is consistent with the lack of experimental evidence for intramolecular oxidative addition reactions in the chromium complexes under consideration. On the other hand, the oxidative addition process is more favorable for the iron complexes. ΔE_{rxn} is predicted to be uniformly lower in the iron complexes than in the chromium complexes, so much that for Fe(CO)₄(C₂Cl₄), C–Cl activation is exoenergetic, consistent with our experimental observations. The cause of such differences in the energy of reaction is due to the differences in the metal basicity. As discussed earlier, the basicity of the metal increases its ability to back-bond, which, in turn, increases the change in hybridization of the olefinic carbons. As a result of the rehybridization of the olefinic carbons, the C–X bond length is expected to increase as a consequence of a weakening (activation) of this bond. The decrease in the calculated C–X bond energy in the bound olefin, relative to the free olefin, correlates well with the elongation of the C–X bond (see Figure 5, top). The weakening of the C–X bond is more pronounced for olefins bound to Fe(CO)₄ than for olefins bound to Cr(CO)₅. As also seen in Figure 5, the calculated elongation of the C–X bond follows the same trend as the calculated energy for the relevant intramolecular oxidative addition reaction.

(54) (a) Weller, B. H.; Miller, M. E.; Grant, E. R. *J. Am. Chem. Soc.* **1987**, *109*, 352. (b) House, P. G.; Weitz, E. J. *Phys. Chem. A* **1997**, *101*, 2988.

(55) Cedeño, D. L.; Weitz, E. J. *Phys. Chem. A* **2000**, *104*, 8011.

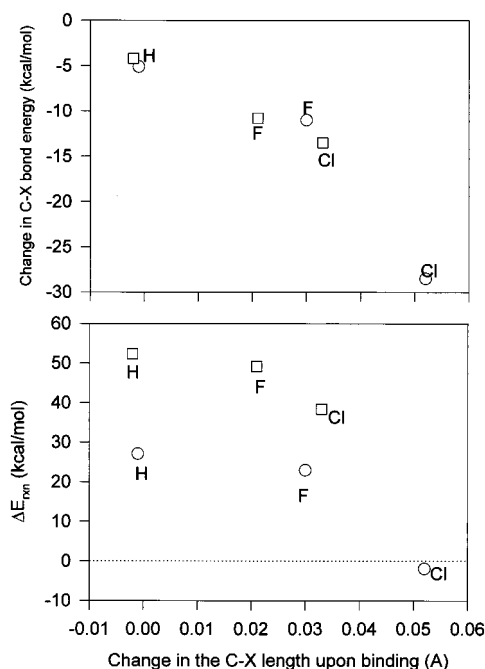


Figure 5. Top: Correlation between the decrease in the calculated C–X bond energy in the bound olefin relative to the free olefin and the elongation of the C–X bond. Bottom: Calculated reaction energy for the oxidative addition reaction $\text{M}(\text{CO})_{x-1}(\text{C}_2\text{X}_4) \rightarrow \text{XM}(\text{CO})_{x-1}(\text{C}_2\text{X}_3)$ as a function of the elongation of the olefin’s C–X bond that occurs upon bonding. Squares (\square) for $\text{M} = \text{Cr}$, $x = 5$; and circles (\circ) for $\text{M} = \text{Fe}$, and $x = 4$.

E. Quantifying Metal–Olefin Interactions: Implications for the DCD Model. The DCD model has been used by chemists to interpret and understand metal–olefin bonding interactions for 50 years. Bonding in the context of this model is pictured as involving the donation of electron density from an olefin to the central metal atom and a synergistic back-donation of electron density from the metal to the antibonding orbital of the olefin. Thus, greater σ donation and/or greater back-bonding should lead to a stronger metal–olefin bond. However, because the DCD model is qualitative, it is not possible to use it to provide a precise prediction as to how changes in the σ donating or π accepting character of a ligand affect the metal–ligand BDE or to make quantitative predictions of BDEs. Nevertheless, with some possible caveats,⁶ it is “conventional wisdom” that the presence of halogen substituents increases the electron withdrawing nature of the olefin ligand to such an extent that back-donation of electron density should be the dominant factor in the bonding interaction.^{6,18} Using our terminology, electron withdrawing olefins increase ΔE_{DCD} , primarily because of an increase in ΔE_{π} . In the context of the DCD model, such a change would contribute to an increase in the BDE of the halogenated Cr–olefin complexes versus the BDE of the analogous ethylene complex. The data in Table 1 make it clear that an increase in the electronegativity (χ)⁵⁶ of the substituents around the double bond *does not* lead to a larger BDE in the compounds under consideration in this study.

The development of reliable theoretical methodologies^{15,20} makes it possible to quantify metal–olefin interactions and the importance of various factors in these interactions. Theoretical studies,^{9,15} including the present work, validate the basic qualitative assumptions of the DCD model: *There is a synergy between electron donation and back-bonding, which enhances*

(56) Pauling scale from: *CRC Handbook of Chemistry and Physics*; Lide, D. R., Ed.; CRC Press: Boca Raton, FL, 1999–2000.

the metal–olefin bonding interaction. However, it is important to note that the DCD model deals explicitly with attractive orbital interactions of the FMOs that lead to bonding (σ and π interactions); that is, $\Delta E_{\text{DCD}} = \Delta E_{\sigma} + \Delta E_{\pi}$. The DCD energy (ΔE_{DCD}) correlates well with the electron withdrawing capability of the olefin. Thus, the DCD model makes an accurate qualitative prediction of the trend in the energy resulting from the FMO bonding interactions, ΔE_{DCD} . However, as the results of the bond energy decomposition analysis demonstrate, there are other factors that contribute to the bond energy. The repulsive energy (ΔE_{steric}) can significantly reduce ΔE_{int} because it can effectively cancel the sum of the attractive orbital interaction terms (ΔE_{DCD} in eq 13) to such an extent that the trend in ΔE_{int} does not reflect the differences in electron withdrawing capability of the olefin substituent, as is evidenced in the ΔE_{int} value for $\text{Cr}(\text{CO})_5(\text{C}_2\text{Cl}_4)$ relative to the ΔE_{int} value for $\text{Cr}(\text{CO})_5(\text{C}_2\text{H}_4)$. Furthermore, the sum of electronic interactions (both attractive and repulsive) does not reproduce the experimental trends in the BDEs in the $\text{Cr}(\text{CO})_5(\text{C}_2\text{X}_4)$ complexes. The calculations show that deformation energies can have a significant effect on bond strengths, and in fact, in at least some systems, such as the present series of complexes, it is the magnitude of the deformation energy, when viewed in relation to the magnitude of ΔE_{int} that establishes the trend in BDEs. Further, though it has been recognized that back-donation can lead to rehybridization, calculations demonstrate that this can be the source of significant deformation energy. The energy cost associated with the geometry changes inherent in this rehybridization can significantly reduce the net energy gained from the attractive orbital interactions. Also, in the case of the halogenated olefin–chromium complexes studied here, there are bonding interactions between non FMOs, which could contribute to the bond energy. Thus, we conclude that an attempt to use the DCD model to predict BDEs, even qualitatively, will fail if the BDEs, or trends in the BDEs, are dominated by factors other than ΔE_{DCD} , as they are for the complexes in this study. This does not imply that the DCD model is incorrect; rather, in some situations, it is being incorrectly applied. However, in the absence of detailed calculations, it is not obvious a priori when BDEs will be dominated by the magnitude of ΔE_{DCD} . Thus, the use of DCD concepts to predict BDEs should be viewed with at least some skepticism.

It should be equally clear that the results of the bond energy decomposition analysis, in combination with other theoretical results, such as orbital overlap integrals, MO energy gaps, and orbital populations, can improve our understanding of metal–ligand bonding at the molecular level through the quantification of the factors contributing to it.

VI. Conclusions

An experimental determination of the Cr–olefin BDE in $\text{Cr}(\text{CO})_5(\text{C}_2\text{Cl}_4)$ (12.8 ± 1.6 kcal/mol) has been performed in the gas phase at 298 K. The experimental result is in agreement with density functional theory (DFT) calculations, which indicate that the Cr– C_2Cl_4 BDE should be significantly lower than the Cr– C_2H_4 BDE in $\text{Cr}(\text{CO})_5(\text{C}_2\text{H}_4)$ (24.8 ± 1.2 kcal/mol). A DFT bond energy decomposition analysis²⁰ of the factors that contribute to the metal–olefin bond energy has been used to obtain quantitative insights into bonding interactions in the relevant complexes. Energy terms that characterize the σ and π electronic interactions are obtained from the analysis and are suitable indicators of the electron donating and accepting character of olefins in a given metal environment. The bond energy decomposition analysis provides strong evidence that the deformation of the moieties involved in metal–olefin

bonding can have a significant effect on the BDEs of metal–olefin complexes. In fact, when viewed in relation to the magnitude of the “bond-snap” energy (ΔE_{int}) and the BDEs, the deformation energy is the determining factor in trends in bond strengths in the homologous series of complexes under study. The major source of the deformation energy in the series $(\text{CO})_5\text{Cr}-\text{C}_2\text{X}_4$ ($\text{X} = \text{H}, \text{F}, \text{Cl}$) involves geometry changes that occur in the olefin on bonding. Although an increase in the electronegativity of the substituents on an olefin increases the back-bonding interaction between the olefin and the metal-centered unsaturated complex, it also leads to increased rehybridization of the olefinic carbon atoms. The change in geometry that results from a rehybridization of these carbon atoms of the olefin involves an “energy cost” that effectively reduces the metal–olefin bond energy. As a result of the olefin rehybridization that occurs upon binding, the C–C and the C–X bonds elongate (with the exception of C–H). The elongation of the C–X bond correlates with a decrease in the C–X bond strength. In all cases, the change in hybridization is more prominent for olefins bound to iron than to chromium: a consequence of differences in metal basicity. The elongation of the C–X bond has more of an effect on the energetics of C–X bond activation for iron complexes because the weakening of the C–X bond is more pronounced than it is in the analogous chromium complexes. Consistent with this explanation, activation of the C–Cl bond in C_2Cl_4 is observed in $\text{Fe}(\text{CO})_4(\text{C}_2\text{Cl}_4)$ but has not been observed in $\text{Cr}(\text{CO})_5(\text{C}_2\text{Cl}_4)$. The lowest energy reaction pathway for $\text{Fe}(\text{CO})_4(\text{C}_2\text{Cl}_4)$ is intramolecular oxidative addition leading to $\text{ClFe}(\text{CO})_4(\text{C}_2\text{Cl}_3)$, while the lowest energy reaction pathway for $\text{Cr}(\text{CO})_5(\text{C}_2\text{Cl}_4)$ is dissociative loss of olefin.

Though the quantitative details of how the size and basicity of the metal and the nature of the ligand(s) affect ΔE_{def} remain to be explored, there is evidence for applicability of the concept of the deformation energy to systems other than metal–olefin complexes.⁴³ The influence of ΔE_{def} on bond enthalpies in iron carbonyl dinitrogen complexes has already been alluded to.⁵⁷ The energy associated with the sum of the σ bonding and π bonding interactions increases in parallel with an increase in the electronegativity of the substituents on the bound olefin. This trend is what is expected on the basis of the DCD model. However, as would also be anticipated, because the DCD model does not explicitly consider the deformation energy or the Pauli repulsive energy, it should not be predictive with respect to systems in which these terms dominate the trend in BDEs. Data from the present study, taken in conjunction with results on other systems,^{9,29,43,58} demonstrate that trends in metal–ligand bond strengths can be explained and understood by quantifying the factors that determine metal–ligand BDEs: the attractive and repulsive electronic interactions and the deformation of the binding moieties.

Acknowledgment. The authors acknowledge support of this work by the National Science Foundation under Grant NSF 97-34891. We thank a reviewer who alerted us to the existence of experimental determination of the structure of the $\text{Cr}(\text{CO})_5$ -(bicycloolefin) complex.

Supporting Information Available: Table with experimental rate constants for recovery of $\text{Cr}(\text{CO})_6$ as a function of $\text{C}_2\text{-Cl}_4/\text{CO}$ pressures ratio in the 288–308 K (PDF). This material is available free of charge via the Internet at <http://pubs.acs.org>.

JA011643X

(57) Cedeño, D. L.; Weitz, E.; Bérces, A. J. *Phys. Chem. A* **2001**, *105*, 3773.

(58) Diefenbach, A.; Bickelhaupt, M.; Frenking, G. *J. Am. Chem. Soc.* **2000**, *122*, 6449.